Contributions to Mineralogy and Petrology (2021) 176:94
https://doi.org/10.1007/s00410-021-01851-z

ORIGINAL PAPER

From peridotite to fuchsite bearing quartzite via carbonation and weathering: with implications for the Pb budget of continental crust

Håkon Austrheim[1] · **Fernando Corfu**[2] · **Christian J. Renggli**[3]

Received: 5 May 2021 / Accepted: 5 October 2021 / Published online: 22 October 2021

Abstract

Extensive carbonation of peridotite results in listvenite, a rock composed of magnesite and quartz. At Gråberget, Røros, SE-Norway, a variably serpentinized peridotite body, surrounded by the Røros schists, a former abyssal sediment displays all stages of transformation of peridotite to quartzite. In this paper we record the sequence of steps in this process by combining the observation of mineral assemblages, textural relationships and geochemistry, and variations in Pb isotopic compositions. Initial serpentinization, a stage that also involved an enrichment in fluid-mobile elements (Pb, Sb and As), was followed by carbonation through CO_2 fluids that formed soapstone, and eventually listvenite. The listvenite grades by decreasing amounts of carbonates into fuchsite bearing quartzite. The carbonates dissolved during supergene alteration and formed pores coated with oxides of Fe, Mn and Ni resulting in a brown rock color. The quartzite displays porous stylolites enriched in Pb, As and Sb and fuchsite with porous chromite grains as the only relicts of the original mineralogy in the peridotite. The dissolution of the carbonate occurred at oxidizing conditions at temperatures below 150 °C, where the solubility of magnesite is higher than that of quartz. Formation of quartzite from peridotite is supported by low REE contents and lack of zircons in the two rock types. The transformation involved enrichment of Pb, coupled with the elimination of Mg and enrichment of Si. This chemical fractionation and selective transfer of elements to the continents is an important mechanism and needs to be taken into account in models of continental evolution.

Keywords Peridotite · Listvenite · Fuchsite–quartzite · Pb-cycle

Abbreviations

SEM	Secondary Electron Microscopy
BSE	Back-scattered Electron Microscopy
CL	Cathodoluminescence
EDS	Energy-dispersive X-ray spectroscopy

Communicated by Daniela Rubatto.

✉ Håkon Austrheim
h.o.austrheim@geo.uio.no

[1] Physics of Geological Processes (PGP), Department of Geosciences, The NJORD Centre, University of Oslo, PO Box 1048, N-0316 Oslo, Norway

[2] Department of Geosciences and CEED, University of Oslo, PO Box 1047, N-0316 Oslo, Norway

[3] Institut für Mineralogie, Westfälische Wilhelms-Universität Münster, Corrensstraße 24, 48149 Münster, Germany

Introduction

The continental crust is generated mainly by partial melting of mantle peridotite, forming a complementary geochemical reservoir to the Earth's depleted mantle (Hofmann 1988). Most elements are enriched in the crust according to their incompatibility during melting of the mantle, although Pb requires alternative mechanisms (Newsom et al. 1986; Hofmann 1988). Peridotites and ultramafic material are also added to the crust through obduction of ophiolites, emplacement and differentiation of magmatic complexes, and extrusion of komatiite lavas. Such material is strongly out of equilibrium at the surface and is susceptible to rapid weathering (Goldich 1938) and carbonation. Already Anderson (1982) suggested that weathering with selective removal of Mg from the crust and its recycling back into the mantle may be an important process for explaining the composition of the continental crust. The contribution of obducted ultramafic material to the composition of the continental crust is difficult to quantify. Geological mapping may provide a

measure of the amount of obducted peridotites, provided that we recognize the products of peridotite weathering. We are, however, ignorant of the amount of ultramafic material obducted through time and the fractionation of elements by weathering is also unknown. Beinlich et al. (2018) showed that the elevated Ni and Cr content of the continental crust compared to andesite may be explained by weathering of 1–2% of ultramafic rocks added to the crust through obduction of ophiolites and as ultramafic lavas. It was noted, however, that the Cr abundance departs from that of Ni, and that Cr is more enriched in the crust, suggesting that the above assumption is not entirely valid. Obducted ophiolites also contain abyssal sediments with exhalative mineralization (SEDEX) and volcanogenic massive sulfide deposits (VMS), where Pb, Zn and Cu are highly enriched relative to crust and mantle. The influence of such material, in particular Pb, on the crustal composition, is not known.

The main mineral in mantle peridotites is olivine (Fo90). Carbonation of olivine along the reaction $(Mg, Fe)_2SiO_4 + 2CO_2 = 2(Mg, Fe)CO_3 + SiO_2$ results in 1 mol of quartz and 2 mol of magnesite with a 10% component of siderite. A lower degree of carbonation of peridotite may give soapstone composed of talc and carbonate. A rock composed of magnesite and quartz with fuchsite is referred to as listvenite (Halls and Zhao 1995). Listvenite has attracted attention as it is commonly associated with lode Au and Ag mineralization together with Au–Sb, Co, Sb, Cu and Ni (Pirajno 2013) and it is thus of economic significance. Listvenites are also of interest as they represent analogs to industrial large scale CO_2 sequestration (Hansen et al. 2005; Falk and Kelemen 2015; Beinlich et al. 2010, 2012). Less attention has been devoted to the formation of quartz from olivine and its consequences for stratigraphic correlations and crustal evolution.

Listvenite occurrences contain fuchsite (Cr–muscovite) in association with quartz and magnesite (Falk and Kelemen 2015; Hinsken et al. 2017). Quartzite colored green by fuchsite occurs worldwide, commonly in association with ultramafites (Cui et al. 2018) and listvenite. Such associations are frequent in the Precambrian, especially in Archean greenstone belts (Nutman et al. 2009). The origin of fuchsite quartzite is disputed and explanations range from hydrothermal alteration / silicification (Martyn and Johnson 1986) to sedimentary mixing of detrital grains from different sources—quartz derived from granitic rocks and chromite from ultramafites (Chatterjee and Das 2004).

In this work we describe the close spatial association of peridotite, listvenite, green quartzite and sediments with exhalative mineralization from the Gråberget south–east of Røros, SE Norway. Based on field relationships combined with whole rock chemistry, mineral chemistry and thermodynamic equilibrium calculations we find that fuchsite quartzite formed from peridotite during a two-stage process: (1) extensive carbonation resulted in a rock composed of magnesite and quartz followed by (2) supergene alteration in which magnesite was dissolved leaving a residue of fuchsite–quartzite.

Geological setting

The Gråberget metaperidotite (Fig. 1) is one of a chain of ultramafic bodies extending northward for more than 200 km from southern Norway along the Caledonides. The main reservoir for Cr in the lithosphere, chromite, is mainly found in peridotite and in particular in dunite, where it may form chromitite bodies. The ultramafic bodies in the Røros area are rich in chromite as evidenced by the many chromite mines in the region (Moore and Hultin 1980). The mines are mainly located in the larger bodies of Feragen and Raudhammeren (Fig. 1a), but mining activity also took place at Gråberget. The peridotites were emplaced along the hyperextended margin of Baltica prior to the Caledonian orogeny (Nilsson and Roberts 2014; Jacob et al. 2017).

The Gråberget body has the shape of a half circle exposed over 0.1 km^2 and is surrounded by Røros schists. The Røros schists contain abundant carbonates and graphite (Rui 1972) and hosts several, previously economically important, deposits of Pb, Zn and Cu interpreted to represent volcanogenic massive sulfides (VMS) or sedimentary exhalative deposits (SEDEX).

Along its southern margin the metaperidotite is converted to soapstone followed by two main lenses of listvenite up to 50 m wide and together several hundred m long (Fig. 1b). The listvenite is brownish with sets of cm-to-dm-thick quartz veins, which stand out on weathered surfaces (Fig. 2b). The volume of quartz veins in listvenite varies from a few % (Fig. 2b) to 50% (Fig. 2c). The quartz veins are confined to the listvenite and are not present in the adjacent rocks. A several-m-thick layer of fuchsite-bearing quartzite is interlayered with the listvenite (Fig. 2d). The peridotite is transected by metagabbroic dikes and intermingled with lenses of metagabbro with a greenschist facies mineralogy.

Methods and sampling

Samples of partly and completely serpentinized peridotite, soapstone, listvenite, fuchsite quartzite, transitional rocks, as well as quartz veins, massive sulfides, Røros schist and metagabbro were collected from the Gråberget body, except for one sample from the border of an ultramafic body 1 km north of Gråberget (GRÅ19–18), which was analyzed to test the generality of our results (Fig. 1; Tables 1 and S1). Thin sections were made from the collected samples and studied by SEM. Mineral chemical analyses were carried out

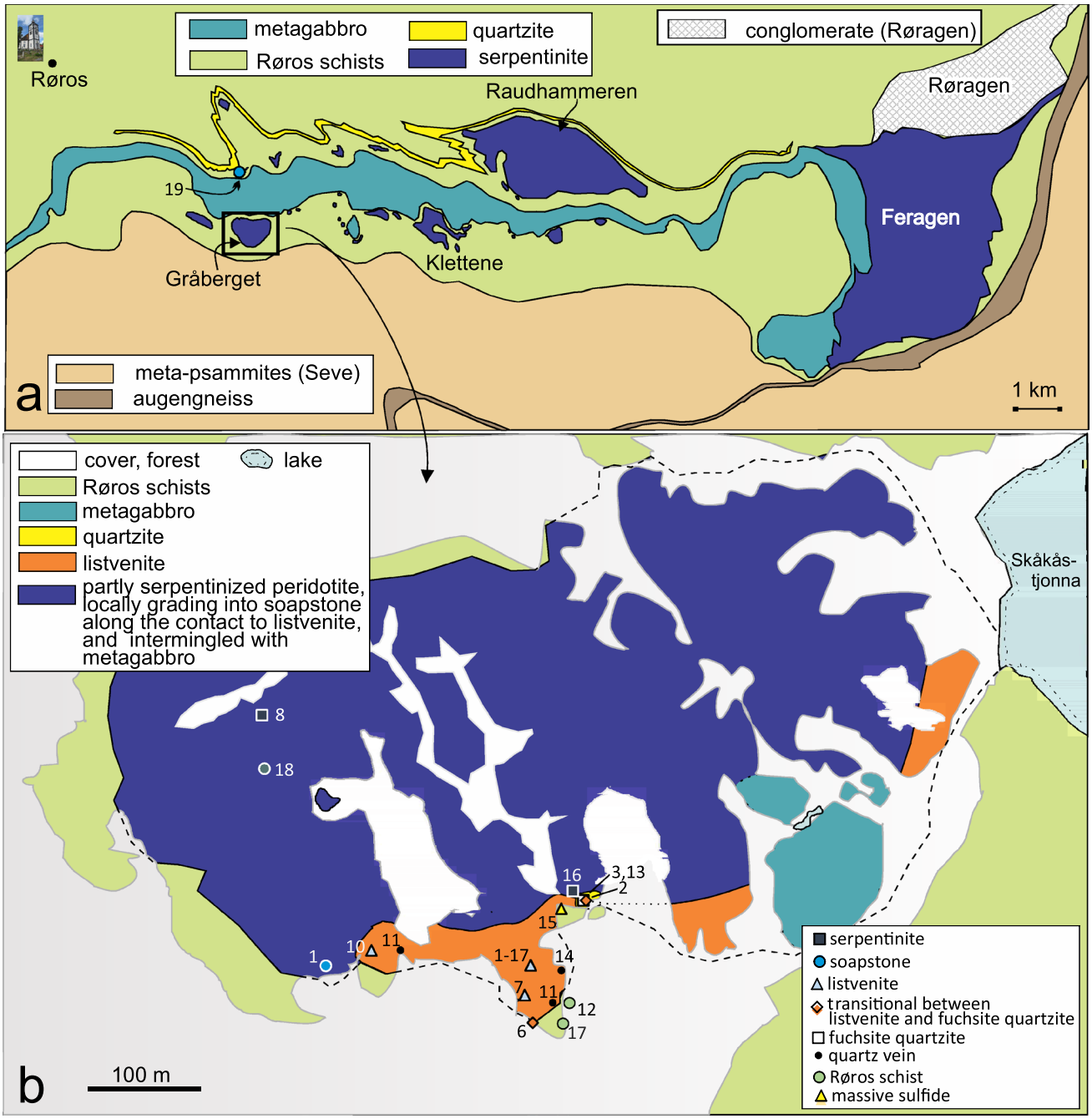

Fig. 1 **a** Geological map showing part of the 200 km long chain of metaperidotites, including the Gråberget, Raudhammaren and Feragen bodies. **b** Geological map of the Gråberget ultramafic body showing the distribution of the main rock types and sample locations (for simplicity the labels are plotted without the prefix GRÅxx-18; see Tables 1 and S1 for details and coordinates)

by a Cameca SX 100 at the Department of Geosciences, University of Oslo (Tables S2 and S3). The analyses were performed at 15 kV and 10 nA beam current. For the Mg-rich carbonates this led to evaporation, as evident by the high totals (Table S2), but this does not affect the relative proportions of the elements of interest. Analyses could not be done with a defocussed beam, because that approach reduced the spatial resolution below the zoning dimensions.

The samples were analyzed for major and trace elements including CO_2 and FeO by Actlabs Laboratories Ltd., using the lithium metaborate / tetraborate fusion ICP whole rock and trace element ICP/MS packages (Table S4). For samples with high concentrations of Pb and Zn (GRÅ15–18 and

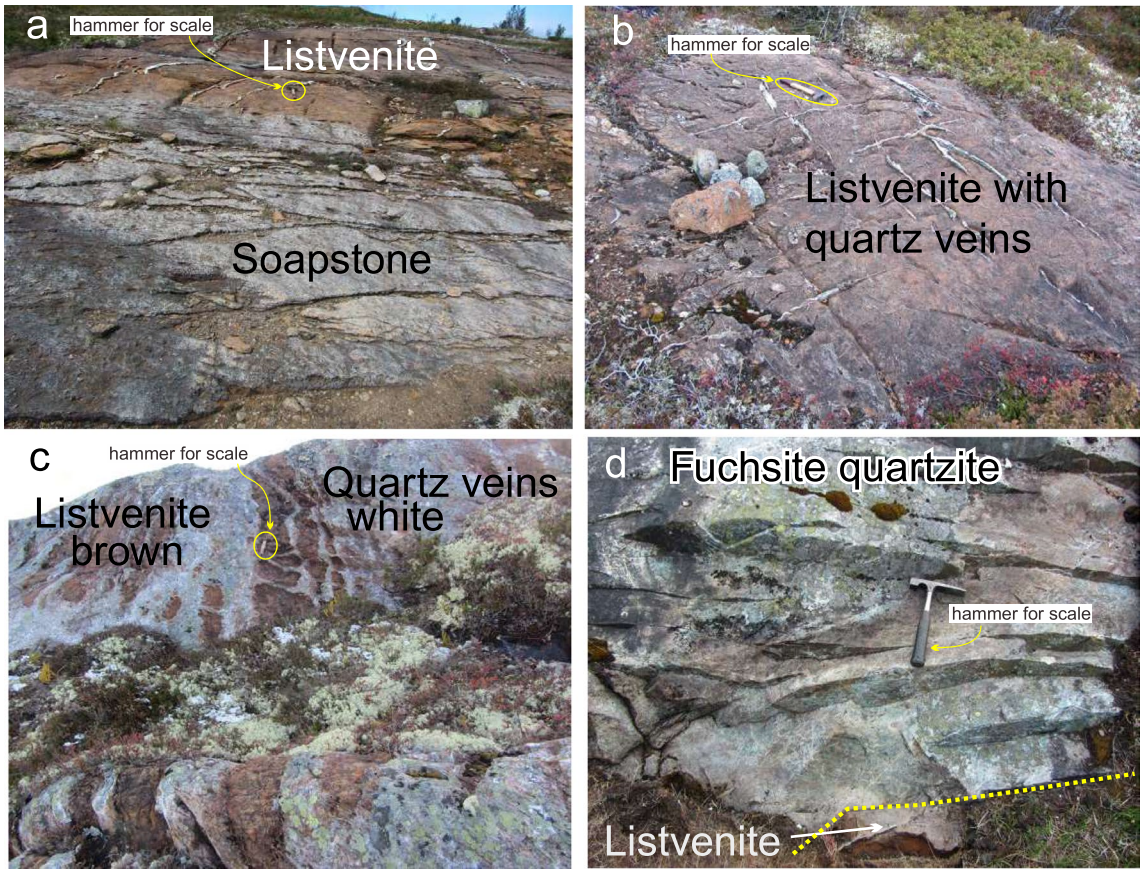

Fig. 2 **a** Contact between soapstone (grey) lower part and listvenite (brown) with quartz veins (upper part). **b** Listvenite with two sets of quartz-veins, which stand out on the weathered surface. **c** Outcrop where quartz veins dominate over listvenite. **d** Fuchsite quartzite in contact with listvenite

GRÅ17–18) these values were obtained using sodium peroxide (Na_2O_2) fusion.

Lead isotopic compositions were determined on a number of samples (Table S5). Titanite and whole-rock samples were dissolved in HF, and pyrite and sphalerite in HCl, using savillex vials on a hot plate. Chromite did not fully dissolve in HCl, nor in HF, but sufficient Pb was leached for the analysis, perhaps from the magnetite components described below. After dissolution the samples (spiked) were re-equilibrated with 3 N HCl before purifying the Pb with HBr in ion exchange resin, followed by cleaning of the U with HNO_3 and 6 N HCl in the same resin. The isotopic compositions were measured with Faraday cups in static mode on a MAT262. Galena was leached shortly with a drop 6 N HCl, and the solution loaded directly with Si–gel on a Re filament for the measurement. The data are normalized with reference to NBS982 Pb.

From serpentinized peridotite to fuchsite bearing quartzite: petrography and mineral chemistry

The *peridotite* at Gråberget is variably serpentinized, ranging in composition from dunite to harzburgite, and is locally intruded by metagabbro. Olivine (Table S3) has a composition of Fo95–97 and contains in average 3540 ppm Ni. In addition to olivine and serpentine the rock contains chromite with ongrowth of magnetite. The chromite is several 100 µm across and displays fractures filled with Cr-bearing magnetite. The serpentine has trails of small magnetite grains formed during the serpentinization process. As in the Feragen body to the east (Fig. 1a; Plümper et al. 2014) serpentine contains chains of µm-sized awaruite (Ni_3Fe). Totally serpentinized peridotite, with a few veins of carbonate (magnesite and dolomite), is present adjacent to the listvenite and soapstone.

Soapstone consisting of carbonate, talc, serpentine and minor chlorite occurs in contact with the listvenite. The soapstone samples, including (GRÅ19–18) collected from the ultramafic body north of Gråberget, contains both talc

Table 1 Sample characteristics and locations

Sample no.	Rock type	Location	Minerals	Microtexture	Comments
GRÅ8–18	Serp perid	Gråberget	ol, srp, chr, awr	Mesh textured	Fo95
GRÅ16–18	Serpentinite	Gråberget	srp, chr, mag, pn		Vein w mgs,dol
GRÅ18–18	Gabbro	Gråberget	plag, amph, ep, chl		Dike
GRÅ1–18	Soapstone	Gråberget	tlc, mgs, chr	Outer rim with voids after mgs	Carbonate rich
GRÅ19–18	Soapstone	Skåkasfjellet	tlc, mgs, qz, chr	Intergrown mgs and tlc	Lens 1 km N of Gråberget
GRÅ1–17	Listvenite	Gråberget	qz, mgs, chr, hem	Zoned mgs (Fig. 3a)	Hem incl. in qz
GRÅ7–18	Listvenite	Gråberget	mgs, dol, qz, pn, py, po, mlr	Sulf. alters to S-free Fe-rich phases	Supergene alteration
GRÅ10–18	Listvenite	Gråberget	qz, mgs, chr		
GRÅ2–18	Transitional	Gråberget	qz, mgs, chr, pn, tlc	Figure 4a,b,c,d	High Ni mgs
GRÅ6–18	Transitional	Gråberget	qz, mgs, gn, sp, py, pn	Partly dissolution of mgs (Fig. 3b)	Hemimorphite after sp
GRÅ14–18	Quartz vein	Gråberget	qz, mgs, pn, py, gn, chr	oxidized sulfides	Grain boundary coating
GRÅ11–18	Quartz vein	Gråberget	qz		
GRÅ3–18	Fuc quartzite	Gråberget	qz, fuc, chr	Stylolite with voids Fig. 5a, b, c, d, e	Stylolite
GRÅ13–18	Fuc quartzite	Gråberget	qz, fuc, mgs		Voids coated w oxide
GRÅ15–18ii	Mass sulf	Gråberget	mgs, dol, gn, sp, py, chr	Veins of Fe-oxid in dol	Supergene alteration
GRÅ12–18	Røros schist	Gråberget	mgs, dol, bio, ms, fsp, zrn, mnz	mgs replaced with oxide	Oxide coating of carbonates
GRÅ17–18A	Røros schist	Gråberget	bio, ms, fsp, bio, zrn, mnz, chr		
GRÅ17–18B	Røros schist	Gråberget	mgs, dol, fsp, bio,ap, zrn,mnz	py and cb alteration (Fig. 3c, d)	Supergene alteration

Abbreviations (after Whitney and Evans 2010): *amp* amphibole, *ap* apatite, *awr* awaruite, *bio* biotite, *cb* carbonate mineral, *chl* chlorite, *chr* chromite, *dol* dolomite, *ep* epidote, *fsp* feldspar, *fuc* fuchsite, *gn* galena, *hem* hematite, *mlr* millerite, *mgs* magnesite, *mnz* monazite, *ms* muscovite, *mag* magnetite, *plag* plagioclase, *pn* pentlandite, *po* pyrrhotite, *py* pyrite, *qz* quartz, *sp* sphalerite, *srp* serpentine, *tlc* talc, *ol* olivine, *zrn* zircon, *Transitional* transitional between listvenite and fuchsite quartzite, *serp* perid serpentinized peridotite, *mass sulf* massive sulfide

and quartz in addition to magnesite and suggests that the soapstone represents an intermediate stage of carbonation on the route from peridotite to listvenite and that listvenitization also affect other ultramafic bodies in the area. The soapstone has developed a 1.5 cm brown zone of post-glacial weathering. The weathered zone is characterized with voids after carbonate. The walls of the voids are coated by rust that locally forms bridges across the voids. Relict carbonates in the weathering zone have developed a rusty surface. Talc contains up to 4 wt.% NiO (Table S2) and is the main carrier of Ni in soapstone.

*S*ample GRÅ18–18 was collected from a *gabbroic dike* in the central part of the peridotite body. The fine grained rock has a greenschist facies mineralogy of abundant (> 60%) epidote and amphibole. Minor phases are titanite, apatite and 10 µm sized zircons.

Listvenite, developed along the southern margin of the body, consists of quartz, chemically zoned magnesite $(Mg_{0.9}Fe_{0.1})CO_3$ to $(Mg_{0.6}Fe_{0.4})CO_3$ (Fig. 3a) and minor amounts of dolomite. Quartz has a smoky appearance due to numerous small inclusions of Fe-oxides. Minor amounts of pyrite, pyrrhotite, pentlandite and millerite are present in GRÅ7–18. The sulfides were oxidized during supergene alteration and the metal ions from the sulfides coat the quartz–quartz grain boundaries. In contact with quartz–quartz grain boundaries carbonates are partly dissolved, while carbonate inclusions in quartz remained intact (Fig. 3b). At the listvenite stage carbonate hosts 2000–3000 ppm Ni, inherited from olivine. Most of the listvenite samples are talc free. Adjacent to oxidized sulfides the carbonate may be totally dissolved, leaving a frame of oxides reflecting the rhombohedral form of the carbonate (Fig. 3c, d).

Quartz veins present in the listvenite contain, in addition to quartz, oxidized sulfides (pentlandite, pyrite, galena), chromite with quartz filled fractures and minor carbonate. The carbonate has a composition corresponding to the Fe-rich rims found in the listvenite. Carbonates are partly or completely dissolved leaving empty or partly filled cavities coated with a brown alteration product of Mn, Pb, Co, Ni, the same material also found along the quartz grain boundaries. Such alteration material, with high Ni/Mg and Si/Mg ratios, is common in laterite formed from ultramafite (Beinlich et al. 2018). The quartz grains range from 10 to 100 µm, similar to the grain size in the listvenite. Raman spectra demonstrate that this is α-quartz.

Quartz veins are characteristic for listvenite worldwide and are typically the locus for metals, in particular gold (Zoheir and Lehmann 2011; Belogub et al. 2017). They are interpreted to form from incoming hydrothermal fluids. At Gråberget the quartz veins are confined to the listvenite (Fig. 2) and the presence of fractured chromite, carbonates

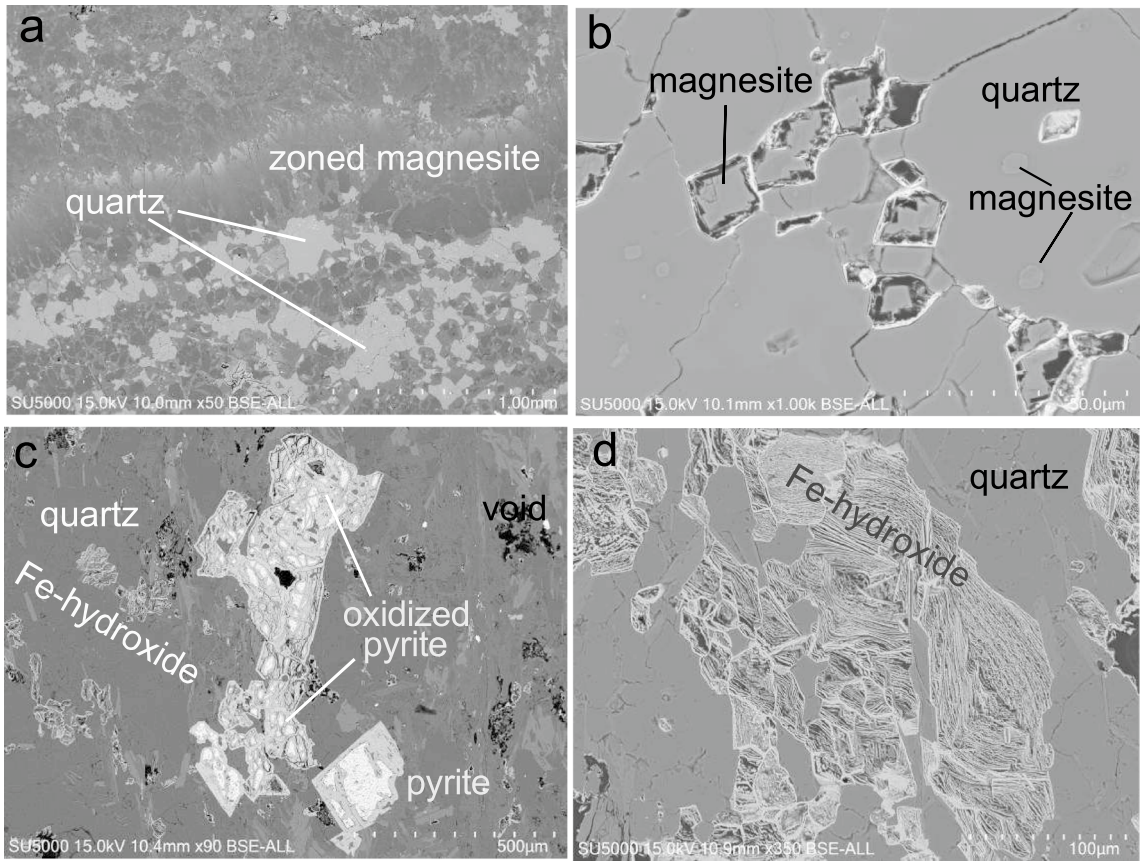

Fig. 3 **a** BSE image of listvenite. Quartz (bright) and zoned magnesite dark to grey. The arrangement of quartz and carbonate may reflect a former mesh texture from the serpentinized peridotite. Sample GRÅ6–18. **b** Magnesite is dissolved with formation of cavities. The cavities are coated on the inside with a bright zone consisting of Fe, Zn and Ni. Note that small inclusions of magnesite (arrows) inside the quartz grain are shielded from the supergene fluid and remained unaltered, while the magnesite grains in contact with grain boundaries show partial dissolution. **c** Supergene alteration of pyrite. Relict pyrite is present in the core of smaller grain. The oxidized part of the sulfide is S-free. The nearby carbonate is dissolved and leaves voids with oxides. **d** Oxide frame after carbonate. Note that the frame reflects the rhombohedral form of the carbonate

and cavities after carbonates supports the interpretation that the quartz veins started as listvenite, but lost most of their carbonate during the supergene alteration.

Rocks transitional between listvenite and fuchsite quartzite with respect to quartz/magnesite ratios display complex structures. Sample GRÅ2–18 (Tables 1, S4) is characterized by a folded, locally discontinuous, foliation defined by chains of small µm-sized carbonate grains, paralleled by fuchsite and alternating with bands, where the carbonate grains are 200 µm across (Fig. 4a). The carbonate grains contain variable Ni contents reaching 1.5 wt.% (Table S2). The form of the zoned carbonates suggests dissolution processes with local Ni enrichment related to the dissolution and reduction of the modal amount of carbonate. Minor amounts of talc are still present in sample GRÅ2–18 supporting its origin from serpentinized peridotite and listvenite.

Fuchsite bearing quartzite carries minor amounts of albite, chromite and chlorite in addition to fuchsite and quartz and displays pressure solution seams in the form of stylolites (Fig. 5a). The stylolites are paralleled by fuchsite and chlorite grains (Fig. 5c–e) and have open pores (Fig. 5a–e) suggesting that they represent zones of high fluid flow. Stylolites with different directions imply that the dissolution is a 3D-feature. The open pores are locally associated with spherulites and an Fe-rich phase (Fig. 5d–e). The compositions of the spherulite and the Fe-rich phases are listed in Table S6. The spherulites contain ca 20 wt.% Pb in addition to 10 wt.% As and between 3 and 3.5 wt.% S. The central parts of the stylolite contain a Fe- and As-rich substance. Carbonates are absent in one sample (GRÅ3–18), but a few grains of magnesite with variable amounts of Ni are present in sample GRÅ13–18. Two textural types of chromite are present—large, fractured and porous grains (Fig. 5a) inherited from the listvenite and small euhedral grains associated with the fuchsite (Fig. 5d) and with pressure solution seams. A survey of the quartzite by CL searching for zircon grains and clastic quartz cores was negative.

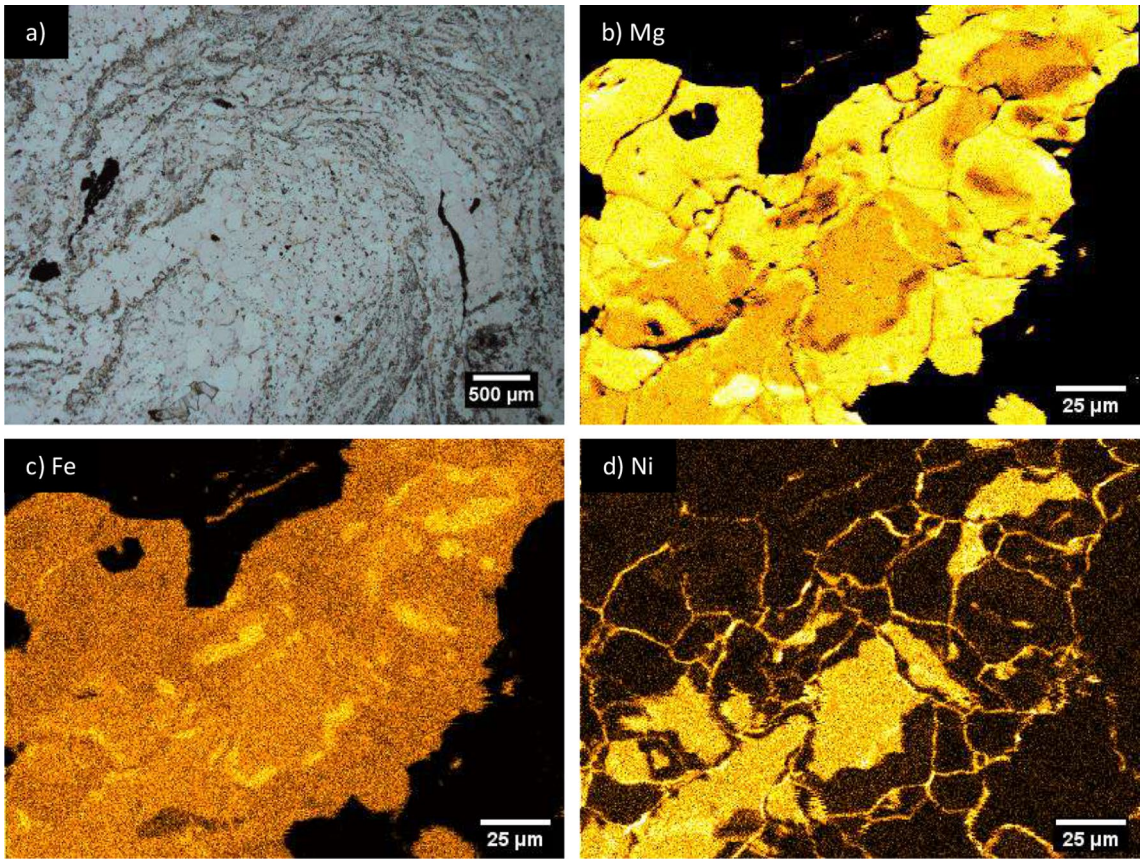

Fig. 4 **a** Photomicrograph of folded solution features in a rock transitional between listvenite and fuchsite quartzite. **b**, **c** and **d** X-ray maps showing the distribution of Mg, Ni and Fe in magnesite–siderite carbonate. Note the local patchy enrichment of the different elements resulting from a dissolution re-precipitation process. The green–red areas in (**c**) correspond to 1.5 wt.% NiO. Note that Ni migrates and forms a network along grain boundaries

Samples of Røros schist adjacent to the fuchsite quartzite contain quartz and feldspar in addition to carbonates (both Fe-rich magnesite and dolomite), micas, abundant Zn–Pb sulfides and oxidized non sulfide Zn and Pb mineralization. In the oxidized zones the magnesite/siderite is replaced by strings of originally Fe oxides. The metals from the oxidized sulfides coat the grain boundaries. Notably, the S from the oxidized sulfide is missing in the altered part of sulfides and along the metal-coated grain boundaries. The magnesite of the Røros schist contains a high siderite content (45%), in magnesite together with traces of Zn (Table S2).

Meter-sized lenses of massive sulfide are present at the contact with the Røros schist. They carry abundant sphalerite, galena and chalcopyrite together with Mg–Fe carbonates and dolomite. The carbonates are dissolved and replaced by oxide strings (Fig. 3d). Chromite grains are abundant suggesting that the host of the massive sulfides are the peridotites.

All rock types of the Gråberget complex, except peridotite and gabbro, contain carbonates that belong to the magnesite–siderite solid solution series (Table S2). Only a few grains of dolomite are present in the serpentinite and listvenite, whereas dolomite becomes abundant in the massive sulfides. High Mg proportions (> 95) are found in the serpentinite, soapstone, listvenite and the transitional samples, which are mostly > 70 (Fig. 6, Table S2). An overall decrease in Ni with decreasing Mg is apparent from Fig. 6. The trend is disrupted by two spikes of high Ni in the transitional rocks, where the Ni reaches 16,000 ppm. As explained above, we interpret the elevated Ni content in the transitional rocks as caused by selective dissolution of magnesite with enrichment of Ni in the remaining carbonate.

Compositional evolution

Whole rock compositions are listed in Table S4. The transformation of peridotite to listvenite decreases most elements, including SiO_2 and MgO, suggesting that listvenitization involves a dilution by addition of CO_2. The MgO/SiO_2 ratio of the soapstone and listvenite varies around the MgO/SiO_2 ratio of the peridotite (Table S4). However, in the transitional rocks, the quartz veins, and the fuchsite quartzite the

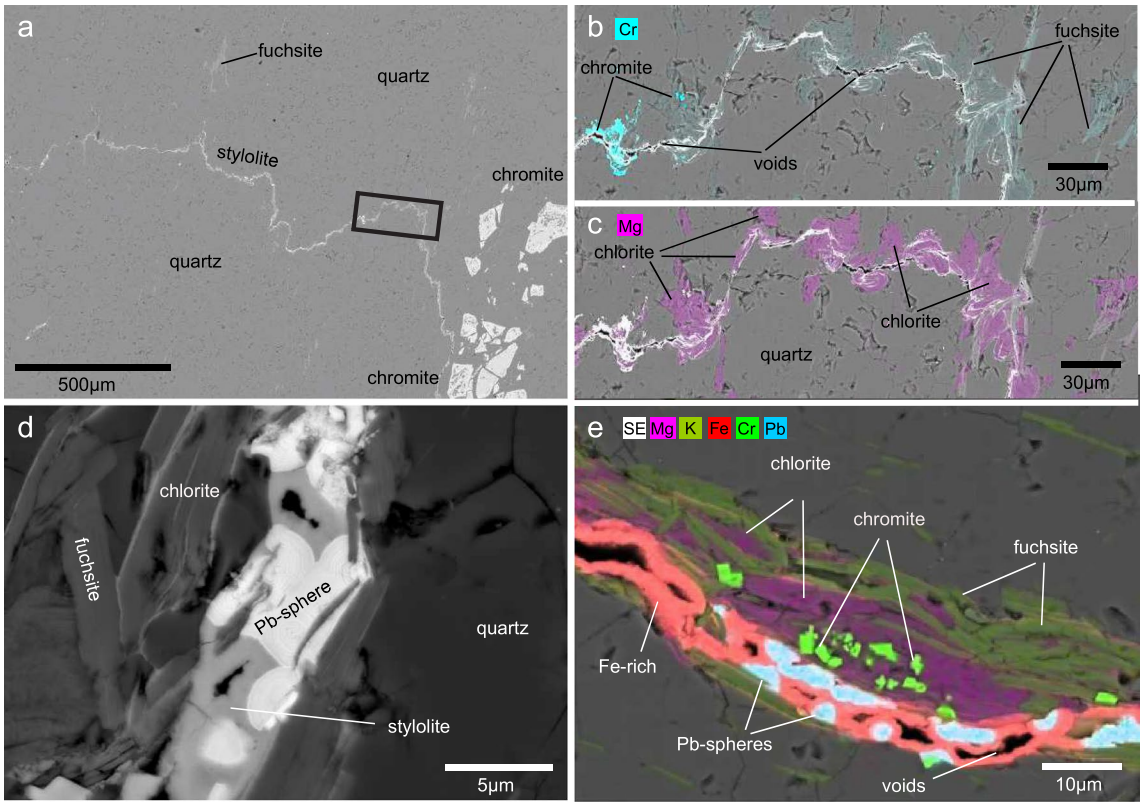

Fig. 5 Stylolites in fuchsite quartzite. **a** BSE image of stylolite. Black rectangle shows the location of the element map shown in **b** and **c**. The stylolite contains voids and consists of a Fe-rich material. The bright grains are a cluster of fragments of a porous chromite grain. **b** Chromium map reflecting fuchsite and chromite along stylolite. **c** Magnesium map. The enrichment of Mg along the stylolite is due to chlorite. **d** BSE image of limb of stylolite. Voids are partly filled by spheres of a Pb-rich material. **e** Composite element map (Mg—lilac, K—light green, Fe—red, Cr—dark green, Pb—blue) over limb of stylolite. The high K-phase is fuchsite: the Mg rich phase is chlorite; small green euhedral grains are chromite. The blue spheres are enriched in Pb. The central part of the stylolite is Fe-rich. Arsenic occurs together with Fe in the central part of the stylolite. EDS analysis documents that the spheres in addition to Fe and Pb also contain As, Sb and minor S

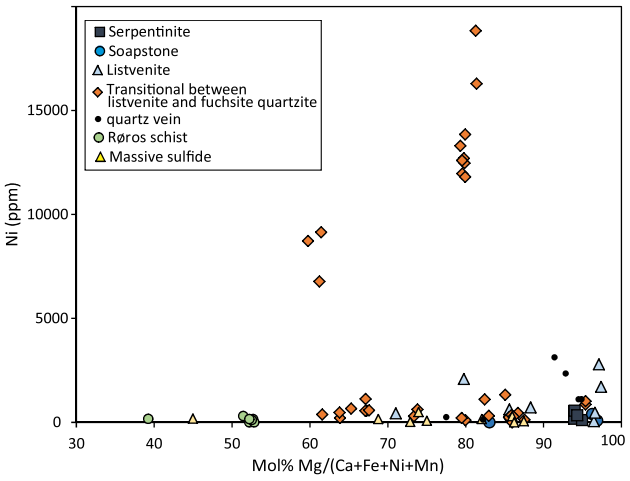

Fig. 6 Variation in Ni (ppm) and Mg content for samples from the Gråberget complex. An overall decrease in Ni with decreasing Mg is apparent. High Ni concentrations in the transitional rocks are interpreted to represent dissolution of magnesite with enrichment of Ni in the remaining carbonate

MgO/SiO_2 ratio is markedly lower. Potassium remains low, but there is a slight increase from 0.01 wt.% in peridotite to 0.14 in the fuchsite quartzite. Zirconium and REE are low (mostly close to or below the detection limits) in ultramafic rocks and the derivatives, but distinctly higher in metagabbro. The gabbro dike contains high CaO (18.2 wt.%) and low SiO_2 (43 wt.%), Na_2O (0.35 wt.%) and K_2O (0.09 wt.%) contents and displays a flat REE pattern with concentration 10 xX chondrite. The chondrite normalized REE-patterns in soapstone and quartzite are very similar, low, and subhorizontal (Fig. 7). Nickel is hosted by olivine in the unaltered peridotite and by awaruite and serpentine in the serpentinite. Talc in the soapstone carries up to 4 wt.% NiO and is the main Ni reservoir. The magnesite in the listvenite contains in average 2500 ppm Ni. A similar Ni-budget was reported by Menzel et al. (2018) related to the formation of listvenite of the Advacade ophiolite, Newfoundland, Canada. Nickel in the quartzite is reduced by 1–2 orders of magnitude compared to the associated peridotite and listvenite.

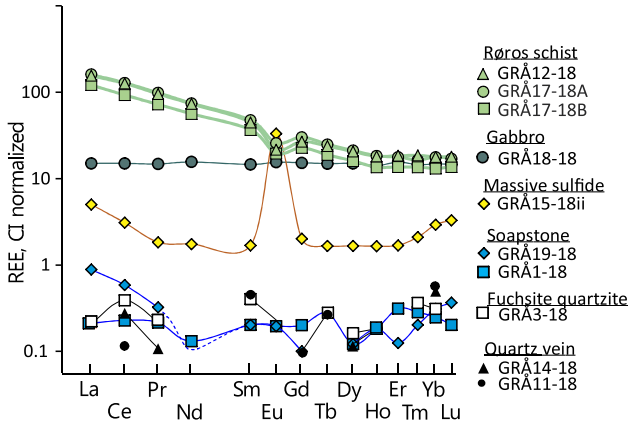

Fig. 7 REE chondrite normalized plot. The data for soapstone, quartzite and quartz veins indicate very low abundances and unfractionated patterns. The results for listvenite were below detection limit (Table S4)

In the primitive mantle normalized spider diagram (Fig. 8) the analyzed rocks show enrichment in the fluid mobile elements Pb, As and Sb. This signature is detectable in the partly serpentinized peridotite, where Sb is enriched 50 × with respect to primitive mantle, and becomes significant in the serpentinite, where Pb reaches 125 ppm with an enrichment factor of 800 × compared to primitive mantle. The listvenite displays abundances similar to the peridotite, but there is a strong increase in the transitional rock and in the quartzite. The low REE content, with Ce mostly below the detection limit of 0.5 ppm, results in extreme Pb/Ce ratios (Table S4).

The Røros schist is compositionally different from the peridotite and its alteration products by containing high Zr, REE, Al_2O_3, while Cr and Ni contents are low. Lead is variably high in the Røros schist (47–1430 ppm). Zinc and Pb are major elements in the massive sulfides.

Lead isotopic compositions

The Pb isotopic compositions obtained in this study (Table S5, Fig. 9) all plot well to the right of the 430 Ma—geochron. This is the typical position of mantle derived magmas produced by sources depleted in Pb relative to U, in contrast to undifferentiated chondritic material which defines the geochron. The data define a broadly correlated array between the compositions of chromite in the peridotite to that of chromite in the Røros schist with the other results plotting in the intervening space. The whole rock values for quartzite, listvenite and serpentinite show higher $^{207}Pb/^{204}Pb$ ratios than the sulfides and titanite in metagabbro and Røros schists. The latter are broadly similar to the compositions measured in the Killingdal deposit (Bjørlykke et al. 1993). The data for various deposits of the Røros district, however, define a shallower oblique line, which is defined by a trend from Pb in 'volcanogenic deposits in an ocean floor environment at the least radiogenic end and sediment-hosted deposits in an intraplate continental environment at the radiogenic end' (Bjørlykke et al. 1993). Most of our new results fit on the latter trend

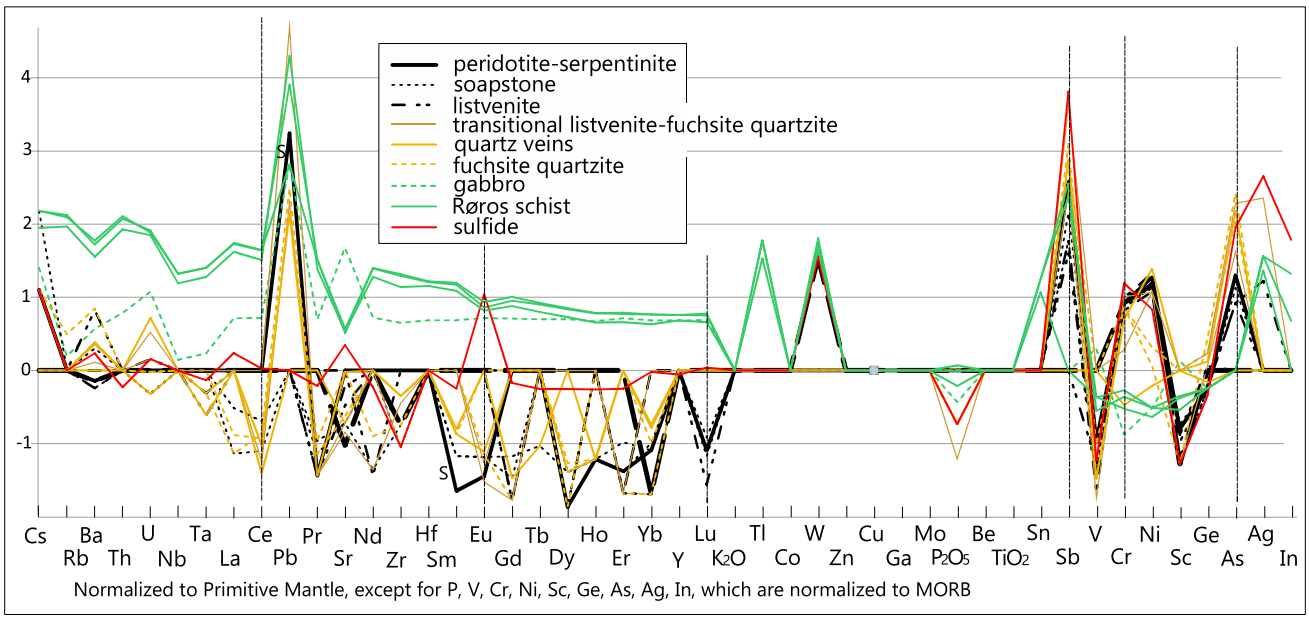

Fig. 8 Multi-element diagram normalized to Primitive Mantle, and to Mid Oceanic Ridge Basalt for P, V, Cr, Ni, Sc, Ge, As, Ag and In (McDonough and Sun 1995). Note the prominent positive spike for Pb

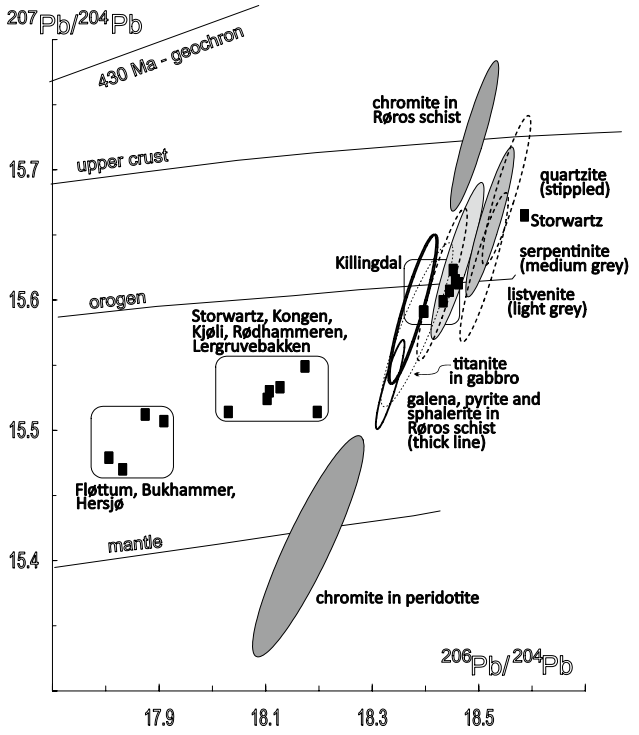

Fig. 9 Lead isotope data for selected minerals and whole rocks from samples representing the main units discussed in the paper and reported in Table S5. The ellipses represent the 2-sigma uncertainties. The curves for mantle, orogen and upper crust are from Zartman and Doe (1981). The squares represent Pb compositions of galena in several deposits of the Røros district (Bjørlykke et al. 1993). The new data span an array from the value for chromite in peridotite, which corresponds to mantle values, to chromite in the Røros schists, which has an upper crustal value. The other data cluster around values typical of orogens and overlap the Pb compositions measured in the Killingdal deposit. They differ from compositions in the other deposits, which are mostly less radiogenic

and probably reflect similar sources, but the chromite in the peridotite is distinct and can be interpreted as the original signature of the parental mantle.

Discussion

Serpentinization and carbonation of the peridotite

Field relations, microtextures and geochemistry point to the formation of the fuchsite quartzite from the Gråberget peridotite via listvenite. Formation of listvenite from peridotite is a well-recognized process, although the tectonic setting for this carbonation remains open. The massive carbonation of the Linnajavri ultramafic body, northern Norway, took place by CO_2 derived from the adjacent carbonate rock (Beinlich et al. 2012). At Gråberget the Røros schist and the massive sulfides are strongly carbonated suggesting that they were carbonated during the same event. It is possible that the carbonation occurred when the ultramafite was still part of the oceanic lithosphere, although listvenite has not been reported from the deep ocean. Serpentinites are known to be enriched in fluid-mobile elements (Deschamps et al. 2011, 2013; Scambelluri 2019). Such enrichment can take place in deformation zones along ridges (Andreani et al. 2014) or during subduction. The fluid-mobile elements in the Gråberget complex must partly have been related to the serpentinization, as serpentinite sample GRÅ16–18 has high Pb, Sb and As contents (Table S4). The metalliferous Røros schist would have been a natural source for the fluid-mobile elements and enrichment of abyssal sediments by hydrothermal solutions may have been the first step in this process (Peucker-Ehrenbrink et al. 1994). Alternatively, the complex and metasediments may have been flushed contemporaneously.

The Pb isotope data obtained in this study support an enrichment of the serpentinite and listvenite by Pb derived from the mineralizing systems that formed the Røros Cu–Zn deposits. The data (Fig. 9) suggest that the original peridotite had a similar Pb composition as the mantle, but the transformation into serpentinite, listvenite and quartzite introduced more radiogenic Pb, broadly similar to that of the ore deposit system. The genesis of the gabbro is somewhat uncertain, but gabbro and diabase dikes are intermingled with peridotites along spreading ridges. Such dikes may be rodingitized and the signature of rodingitization (high CaO and low SiO_2, Na_2O and K_2O) in the Gråberget gabbro suggests that the gabbro formed during oceanic crust formation and became rodingitized during serpentinization of the peridotite. The transfer of lead from the metalliferous Røros schist to the serpentinites likely took place in the oceanic crust. These units were not affected by subduction, but potential partial reworking during Caledonian thrusting and subsequent denudation may have occurred.

The massive sulfides are rich in Cr but low in Al_2O_3 and Zr, which suggest that they formed from ultramafic protoliths. Interestingly the analyzed sample of massive sulfide displays a U shaped REE pattern with a strong positive Eu-anomaly (Fig. 7), characteristic for abyssal massive sulfides (Zeng et al. 2015).

The listvenite-to-quartzite transformation

Silica-rich listvenite, also named birbirite, is known from a number of places (Stanger 1985; Akbulut et al. 2006; Menzel 2020; Boskabadi et al. 2020). Birbirite is mainly interpreted to have formed by silicification of listvenite. However, thermodynamic modeling (Klein and Garrido 2011) shows that birbirite can form by dissolution of carbonate. Our observations support the models by Klein and Garrido (2011). It is well known that carbonates can dissolve close to the Earth's surface to form karst terrains. The microtextures

suggest that the carbonates are dissolved during oxidation of the sulfides when sphalerite is transformed to hemimorphite and pyrite to Fe-hydroxide. Interestingly, non-sulfide Zn–Pb deposits form karst fills (Hitzman et al. 2003). The sulfides present in the listvenite, quartz veins and quartzites loose the S during a process referred to as supergene alteration. We find that the supergene process must have played a role in the dissolution of carbonates, as metals from the oxidized sulfides are deposited inside the cavities after carbonates and on grain boundaries (Fig. 5). Stylolites are also known to develop close to the surface of the Earth (Koehn et al. 2012) and we relate the listvenite to quartzite formation as a near surface process.

The removal of carbonates from listvenite will produce a quartz rich rock, in a process that started from peridotite. A consequence of this is that supergene alteration may also be a rock forming process, in this case participating in the formation of quartzite from peridotite.

Pores coated with oxides that extend out along quartz–quartz grain boundaries suggest that grain boundaries act as transport channels for fluids that can dissolve the carbonate and leave behind Fe-oxides. Stylolites present in the carbonate free quartzite are porous and locally filled with spheres of Pb-rich material (Fig. 5). Stylolites are known to be porous and active overpressure conduits for corrosive and mineralizing fluids (Bruna et al. 2019; Heap et al. 2014; Martin-Martin et al. 2016). This may indicate that Pb was introduced along the stylolite, possibly from the surrounding Røros schist. However, we cannot exclude that the stylolites were conduits for material leaving the system and that the porosity was due to overpressured fluids from carbonate dissolution. In this case the Pb may have been deposited from this fluid and originated in the listvenite. Thus, Pb may have originated in the peridotite or been added to the peridotite during the carbonation event. Stylolites suggest that pressure solutions have been active in the complete removal of carbonates and the early formed pores. The discontinuous foliation and folding observed in a rock that has lost most of its carbonate (Fig. 4) point to a more complex process of combined dissolution, replacement and deformation. The large volume reduction and pore formation may lead to collapse of the rock. During such a process local high stress points with enhanced dissolution will develop with a strong feed-back between dissolution and fluid transport.

The formation of the fuchsite quartzite from the carbonate-bearing listvenite rock requires the reaction of the listvenite with a fluid capable of dissolving the carbonates more than quartz. This process follows an initial carbonate forming CO_2-metasomatism, which occurs at low temperature < 300 °C (Halls and Zhao 1995; Falk and Kelemen 2015). Similarly, dissolution of the carbonates also occurs at low temperature. For example, serpentinization and carbonation reaction path models suggest that at temperatures below 150 °C carbonate is dissolved. In contrast, above 200 °C the final carbonation step is followed by the dissolution of quartz (Klein and Garrido 2011).

The composition of the carbonate dissolving fluid is not directly constrained. However, we observe the oxidation of pyrite to Fe-hydroxide texturally associated with the carbonate dissolution (Fig. 5), for example through the following reaction:

$$FeS_2 + 3.75O_2 + 2.5H_2O = FeO \times OH + 2SO^{2-}_{4(a)} + 4H^{+}_{(a)} \quad (1)$$

The presence of sphalerite oxidized to hemimorphite further suggests oxidizing conditions. The relative solubilities of the carbonates and quartz constrain the nature of the fluid. We describe the dissolution of $MgCO_3$ (magnesite) and SiO_2 (quartz) in a hydrothermal fluid using hydrolysis reactions (Bowers et al. 1984). The solubility of the carbonates is evaluated at oxidizing conditions, as suggested by the oxidized sulfides, and at neutral pH. These conditions are associated with carbonation and serpentinization environments of ultramafic rocks (Bruni et al. 2002; Klein and Garrido 2011). At these conditions sulfur is dissolved as the sulfate anion (SO_4^{2-}) and carbon as bicarbonate (HCO_3^{-}). Here we compare the simple dissolution of magnesite (Eq. 2), with the dissolution of magnesite in the presence of sulfate from the pyrite oxidation (Eqs. 3 and 4), and the dissolution of quartz (Eq. 5). The subscript $_{(a)}$ denotes that the species is dissolved in an aqueous solution. We calculate the equilibrium constants of the reactions (1) to (5) using the software package HSC Chemistry 9 (2018).

$$MgCO_3 = CO^{2-}_{3(a)} + Mg^{2+}_{(a)} \quad (2)$$

$$MgCO_3 + SO^{2-}_{4(a)} + 2H^{+}_{(a)} = Mg^{2+}_{(a)} + HCO^{-}_{3(a)} + HSO^{-}_{4(a)} \quad (3)$$

$$MgCO_3 + SO^{2-}_{4(a)} + 2H^{+}_{(a)} = Mg^{2+}_{(a)} + HCO^{-}_{3(a)} + SO^{2-}_{4(a)} + H^{+}_{(a)} \quad (4)$$

$$SiO_2 = SiO_{2(a)} \quad (5)$$

The equilibrium constants of these reactions are shown in Fig. 10 as a function of temperature from 0 to 300 °C and the calculation results are included in the supplement (Table S7). We observe that in the presence of sulfate in the solution magnesite is more soluble than quartz over the entire temperature range. For example, at 100 °C the equilibrium constant of the dissolution reaction of magnesite (3) is logK = 6, nine orders of magnitude higher than that of the quartz dissolution (5) with logK = – 3.2. These thermochemical considerations support our textural observations that the fuchsite quartzite formed from the dissolution of

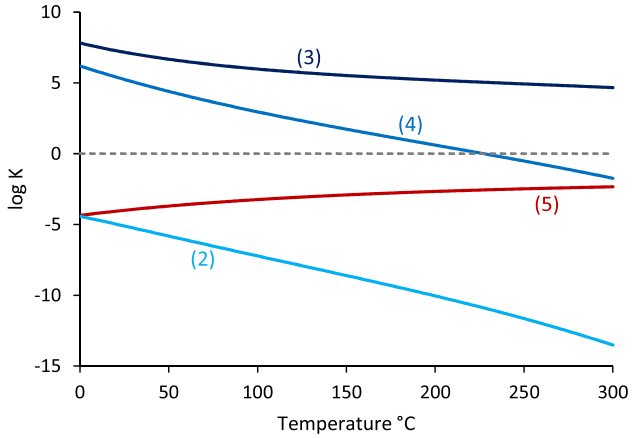

Fig. 10 Logarithms of the equilibrium constants of reactions (2) to (5) at atmospheric pressure and temperatures of 0–300 °C

the carbonates in the listvenite, and are in agreement with previous reaction path models (Klein and Garrido 2011).

The geochemical data support our model as the REE element patterns in peridotite, listvenite and quartzite are identical. Zircon, ubiquitous in sedimentary quartzites, is absent in the fuchsite quartzite as in peridotite and listvenite. Chromite is a key mineral in tracing the transition from peridotite to quartzite as it is the only mineral that remains from the peridotite. The porous nature of the chromite grains observed in the quartzite suggests that the chromite was dissolved providing the Cr to form fuchsite and associated small euhedral chromite crystals. It is suggested that the dissolution relates to the stylolite formation as the small euhedral crystals are located along these structures (Fig. 5e). Fragmented chromite grains can be followed from the listvenite into the quartzite which is also unlikely if the quartzite formed by a sedimentary process.

Implications for the composition of the continental crust

Fuchsite quartzites are present world-wide and are particularly frequent in Precambrian and Archaen terrains (Nutman et al. 2009). India hosts a number of fuchsite quartzites and, interestingly, Radhakrishna and Naqvi (1986) noted that the sediments are rich in Ni and Cr, although the area lacks an obvious source in the form of peridotite. A model for fuchsite–quartzite formation as outlined here can explain this apparent paradox. Understanding how this process influences the crustal composition requires estimating the amount of mantle rocks obducted and the way carbonation and weathering fractionate elements. Chromium and Ni are highly enriched in peridotites relative to continental crust, but these two elements behave differently during listvenite formation—Ni follows Mg and enters carbonate, while Cr remains in chromite grains although Cr is mobilized locally during carbonat dissolution. The diverging paths of these two elements may explain why Cr to a higher degree then Ni remains in the continental crust (Beinlich et al. 2018). Removal of carbonates will not only remove the added CO_2, but also the 50 wt.% of MgO originally present in peridotite. A central issue is the fate of Mg during the described process. As we have not found potential deposits of Mg in the studied region we assume that Mg was lost to rivers and the ocean. Shen et al. (2009) concluded from Mg-isotope systematics that the continental crust is too Si-rich and Mg-poor and argues that this is due to Mg loss during weathering of basalt. Clearly the process described here, where the transformation of peridotite to quartzite results in an increased Si/Mg, provides a plausible explanation for the finding of Shen et al. (2009).

The enrichment of fluid-mobile elements in many abyssal peridotites (Deschamps et al. 2011; Andreani et al. 2014; Scambelluri et al. 2019), also obvious in the peridotite and serpentinite at Gråberget, is a feature that can be traced through to the quartzite, where the enrichment is accentuated. A central problem of mantle evolution and crustal growth relates to the anomalous enrichment of Pb in the continental crust (Chauvel et al. 1995). Lead is a moderately compatible element behaving like Ce (Hofmann et al 1986; Newsom et al. 1986; Hofmann 1988). During melting they should be retained in the mantle preferentially to the more incompatible elements Th, and U. If Pb was transferred to the crust in the same rate as Ce, the U/Pb ratio of the crust should be two and four orders higher than primordial mantle and depleted mantle, respectively, but they have been shown to be of the same order (Peucker-Ehrenbrink et al. 1994). The Pb/Ce ratio is also found to be much higher in the continental crust than anticipated based on their compatibility during melting. These relationships have been explained as the result of hydrothermal extraction of Pb from the basalt and its storage into the abyssal sediments (Chauvel et al. 1995; Peucker-Ehrenbrink et al. 1994). The next step, the transfer of the Pb from the sediments to the continental crust is explained by these authors by the dehydration of the oceanic crust and sediments during subduction, the fluid also carrying Pb into the mantle wedge, which upon melting forms continental crust (Chauvel et al. 1995; Peucker-Ehrenbrink et al. 1994). Our observations at Gråberget prove, however, that altered and Pb-enriched oceanic lithosphere can be transferred directly to the continent with no need of the subduction zone circuit. The fuchsite quartzite displays extremely high Pb/Ce, Pb/Th and Pb/U ratios (Fig. 8; Table S4). In addition, the Pb isotope ratios in the various units are consistent with an origin from depleted mantle and hydrothermal interactions in the oceanic lithosphere before being tectonically inserted in the continental crust. Obduction of the massive sulfides and sediments (Røros schist) also add Pb to the continental crust without melting.

Conclusions

The Gråberget ultramafic body, near Røros in the Scandinavian Caledonides, exemplifies the transition from peridotite to quartzite through a sequence of stages involving serpentinization, carbonation though the influx of CO_2 forming soapstone, and at a more advanced stage listvenite. Serpentinization caused the enrichment in fluid-mobile elements, including Pb. The enrichment is also recorded in the surrounding Røros schists, a massif sulfide deposit-hosting back-arc assemblage. Subsequent loss of Mg from the listvenite led to transitional rocks with an end member represented by essentially pure fuchsite quartzite. The derivation of the quartzite from peridotite is supported by the presence of residual chromite and the absence of detrital zircon in the former. At Gråberget, the transformation from peridotite to quartzite can be followed in detail through the observation of mineral assemblages, textural relationships and geochemistry, combined with variations in Pb isotopic compositions. The reaction of listvenite with a fluid which dissolves preferentially the carbonates rather than quartz is modeled for temperatures between 0 and 300 °C, taking into consideration the fact that the reactions occurred at oxidizing conditions which dissolved sulfides and liberated S. The enrichment of Pb, coupled with the elimination of Mg and enrichment of Si was linked to the obduction of mantle peridotites in ophiolites and in hyperextension assemblages. This transfer represents an important mechanism in the formation and composition of the continental crust and needs to be taken into account in models of continental evolution.

Supplementary Information The online version contains supplementary material available at https://doi.org/10.1007/s00410-021-01851-z.

Acknowledgements HA thanks Lisa De Ruiter, Ole Ivar Ulven and Kristina Dunkel for assistance in the field. Discussion with Andreas Beinlich and Andrew Putnis during the progress of this work is greatly acknowledged. Muriel Erambert and Siri Simonsen helped during EMP and SEM work. The paper improved from constructive and thoughtful reviews by M. Menzel and an anonymous reviewer. Daniela Rubatto handled the manuscript in a swift and thorough way and provided useful suggestions and corrections. FC acknowledge a "Småforsk" grant from the Geology Department. HA acknowledge funding from the ITN "Nanoheal" and a Humboldt prize that made this work possible. The detailed mapping of the listvenite was possible through funding from Norwegian Science Foundation (NFR) to the NATSORB-project. CR is funded by the Deutsche Forschungsgemeinschaft (DFG, German Research Foundation) - 442083018.

Funding Open access funding provided by University of Oslo (incl Oslo University Hospital).

References

Akbulut M, Piskin Ø, Karayigit AI (2006) The genesis of the carbonatized and silicified ultramafics known as listvenites: a case study from the Mikaliccik region (Eskisehir) NW Turkey. Geol J 41:557–580

Anderson AT (1982) Parental basalts in subduction zones: implications for continental evolution. J Geophys Res 87(B8):7047–7060

Andreani M, Escartin J, Delacour A, Ildefonse B, Godard M, Dyment J, Fallick AE, Fouquet Y (2014) Tectonic structure, lithology, and hydrothermal signature of the Rainbow massif (Mid-Atlantic Ridge 36°14'N). Geochem Geophys Geosyst. https://doi.org/10.1002/2014GC005269

Beinlich A, Austrheim H, Glodny J, Erambert M, Andersen TB (2010) CO_2 sequestration and extreme Mg depletion in serpentinized peridotite clasts from the Devonian Solund basin, SW-Norway. Geochim Cosochim Acta 74:6935–6964

Beinlich A, Plümper O, Hövelmann J, Austrheim H, Jamtveit B (2012) Massive serpentinite carbonation at Linnajavri, N-Norway. Terra Nova 24:446–455

Beinlich A, Austrheim H, Mavromatis V, Grguric B, Putnis CV, Putnis A (2018) Peridotite weathering is the missing ingredient of Earth's continental crust composition. Nat Com. https://doi.org/10.1038/s41467-18-03039-9

Belogub EV, Melekestseva IY, Novoselov KA, Zabotina MV, Tretyakov V, Zaykov A, Yuminov AM (2017) Listvenite-related gold deposits of the South Urals (Russia): a review. Ore Geol Rev 85:247–270

Bjørlykke A, Vokes FM, Birkeland A, Thorpe RI (1993) Lead isotope systematics of strata-bound sulfide deposits in the Caledonides of Norway. Econ Geol 88:397–417

Boskabadi A, Pitcairn IK, Leybourne MI, Teagle DAH, Cooper MJ, HadizadehBezenjani RN, Bagherzaeh RM (2020) Carbonation of ophiolitic ultramafic rocks: Listvenite formation in the Late Cretaceous ophiolites of eastern Iran. Lithos 325–353:105307

Bowers TS, Jackson KJ, Helgeson HC (1984) Equilibrium activity diagrams. Springer-Verlag, Berlin Heidelberg

Bruna P-O, Lavenu APC, Matonti C, Bertotti C (2019) Are stylolites fluid-flow efficient features? J Struct Geol 125:270–277

Bruni J, Canepa M, Chiodini G, Cioni R, Cipolli F, Longinelli A, Marini L, Ottonello G, Zoccolini MV (2002) Irreversible water-rock mass transfer accompanying the generation of the neutral, Mg-HCO_3 and high-pH, Ca-OH spring waters of the Genova province, Italy. Appl Geochem 17:455–474

Chatterjee RS, Das S (2004) Tattekere conglomerate-quartzite association: origin and stratigraphic position of a disputed Archean formation in the supracrustals of Karpataka, India. J Asian Earth Sci 23:247–261

Chauvel C, Goldstein SL, Hofmann AW (1995) Hydration and dehydration of oceanic crust controls Pb evolution in the mantle. Chem Geol 126:65–75

Cui X-H, Zhai M-G, Guo J-H, Zhao L, Zhu X-Y, Wang H-Z, Huang G-Y, Ge S-S (2018) Field occurrences and Nd isotopic characteristics of the meta-mafic-ultramafic rocks from the Caozhuang

complex, eastern Hebei: Implications for the early Archean crustal evolution of the North China craton. Precamb Res 310:425–442
Deschamps F, Godard M, Guillot S, Andriani M, Hattori K (2011) Serpentinites act as sponges for fluid-mobile elements in abyssal and subduction zone environments. Terra Nova 2:171–178
Deschamps F, Godard M, Guillot S, Hattori K (2013) Geochemistry of subduction zone serpentinites: a review. Lithos 178:96–127
Falk ES, Kelemen PB (2015) Geochemistry and petrology of listvenite in the Semail ophiolite, Sultanate of Oman: complete carbonation of peridotite during ophiolite emplacement. Geochim Cosmochim Acta 160:70–90
Goldich SS (1938) A study in rock weathering. J Geol 46:17–58
Halls C, Zhao R (1995) Listvenite and related rocks: perspectives on terminology and mineralogy with reference to an occurrence at Cregganbaun, Co., Mayo, Republic of Ireland. Mineral Deposita 30:303–313
Hansen LD, Dipple GM, Gordon TM, Kellett DA (2005) Carbonated serpentinite (Listwanite) at Atlin, British Columbia: a geological analogue to carbon dioxide sequestration. Canad Min 43:225–239
Heap MJ, Baud P, Reuschle T, Meredith PG (2014) Stylolites in limestones: Barriers to fluid flow? Geology 42:51–54
Hinsken T, Bröcker M, Strauss G, Bulle F (2017) Geochemical, isotopic and geochronological characterization of listvenite from the Upper Unit on Tinos, Cyclades, Greece. Lithos 282–283:281–297
Hitzman MW, Reynolds NA, Sangster DF, Allen CR, Carman CE (2003) Classification, genesis, and exploration guides for nonsulfide zinc deposits. Econ Geol 98:685–714
Hofmann AW (1988) Chemical differentiation of the earth: the relationship between mantle, continental crust, and oceanic crust. Earth Planet Sci Lett 90:297–314
Hofmann AW, Jochum KP, Seufert M, White WM (1986) Nd and Pb in oceanic basalts: New constraints on mantle evolution. Earth Planet Sci Lett 79:33–45
HSC Chemistry 9 [Computer software] (2018) Metso:Outotec. http://www.mogroup.com/portfolio/hsc-chemistry/
Jacob J, Alsaif M, Corfu F, Andersen TB (2017) Age and origin of thin discontinuous gneiss sheets in the distal domain of the magma-poor hyperextended pre-Caledonian margin of Baltica, southern Norway. J Geol Soc 174:557–571
Klein F, Garrido CJ (2011) Thermodynamic constrains on mineral carbonation of serpentinized peridotite. Lithos 126:147–160
Koehn D, Ebner M, Renard F, Toussaint R, Passchier CW (2012) Modelling of stylolite geometries and stress scaling. Earth Planet Sci Lett 341–344:104–113
Martin-Martin JD, Gomez-Rivas E, Gomez-Gras D, Trave A, Ameniro R, Koehn D, Bons P (2016) Activation of stylolites as conduits for overpressured fluid flow in dolomitized platform carbonates. Geol Soc Lond Spec Pub. https://doi.org/10.1144/SP459.3
Martyn JE, Johnson GJ (1986) Geological setting and origin of fuchsite – bearing rocks near Menzies, Western Australia. J Earth Sci 33:1–18
McDonough WF, Sun SS (1995) The composition of the Earth. Chem Geol 120:223–235
Menzel M (2020) Brittle deformation of carbonated peridotite-insight from listvenites of the Semail Ophiolite (Oman Drilling Project Hole BT1B). J Geophys Res Solid Earth. https://doi.org/10.1029/2020JB020199
Menzel MD, Garrido CJ, Sanchez-Vizcaino L, Marchesi C, Hidas K, Escayola MP, Delgado Huertas A (2018) Carbonation of mantle peridotite by CO2-rich fluids: formation of listvenites in the Advacate ophiolite complex Newfoundland, Canada). Lithos 323:238–261
Moore AC, Hultin I (1980) Petrology, mineralogy and origin of the Feragen ultramafic body, Sør-Trøndelag, Norway. Norsk Geol Tidsskrift 60:235–254
Newsom HE, White WM, Jochum KP, Hofmann AW (1986) Siderophile and chalcophile element abundance in oceanic basalts, Pb isotope evolution and growth of the Earth's core. Earth Planet Sci Lett 80:299–313
Nilsson L-P, Roberts D (2014) A trail of ophiolitic debris and its detritus along the Trøndelag-Jämtland border: correlations and palaeogeographical implications. Norges Geol Unders Bull 453:29–41
Nutman AP, Friend CRL, Paxton S (2009) Detrital zircon sedimentary provenance ages for the Eoarchaean Isua supracrustal belt southern West Greenland: Juxtaposition of an imbricated ca 3700 Ma juvenile arc against an older complex with 3920–3760 Ma components. Precamb Res 172:212–233
Peucker-Ehrenbrink B, Hofmann AW, Hart SR (1994) Hydrothermal lead transfer from mantle to continental crust: the role of metalliferous sediments. Earth Planet Sci Lett 125:129–142
Pirajno F (2013) Effects of metasomatism on mineral systems and their host rocks: alkali metasomatism, skarns, greisens, tourmalinites, rodingites, black wall alteration and listvenites. In: Harlov DE, Austrheim H (eds) Metasomatism and chemical transformation of rock: the role of fluids in terrestrial and extraterrestrial processes. Lecture notes in earth system sciences. Springer, Berlin, pp 203–253
Plümper O, Beinlich A, Bach W, Janots E, Austrheim H (2014) Garnet within geode-like serpentinite veins: Implications for element transport, hydrogen production and life-supporting environment formation. Geochim Cosmochim Acta 141:454–471
Radhakrishna BP, Naqvi SM (1986) Precambrian continental crust of India and its evolution. J Geol 94:145–166
Rui IJ (1972) Geology of the Røros District, south-eastern Trondheim Region with a special study of the Kjøliskarvene-Holtsjøen Area. Norsk Geol Tidskrift 52:1–21
Scambelluri M, Cannao E, Cilio M (2019) The water and fluid-mobile element cycles durig serpentinite subduction. Eur J Mineral 31:405–428
Shen B, Jacobsen B, Lee Cin-Ty A, Morton DM (2009) The Mg isotope systematics of granitoids in continental arcs and implications for the role of chemical weathering in crust formation. Proc Natl Acad Sci USA 106:20652–20657
Stanger G (1985) Silicified serpentinite in the Semail nappe of Oman. Lithos 18:13–22
Whitney DL, Evans BW (2010) Abbreviation for names of rock-forming minerals. Am Min 95:185–187
Zartman RE, Doe BR (1981) Plumbotectonics—the model. Tectonophys 75:135–162
Zeng Z, Ma Y, Yin X, Selby D, Kong F, Chen S (2015) Factors affecting the rare earth element composition in massive sulfides from deep sea hydrothermal systems. Geochem Geophys Geosyst 16:2679–2693. https://doi.org/10.1002/2015GC005812
Zoheir B, Lehmann B (2011) Listvenite-lode association at Barramiya gold mine, Eastern Desert. Egypt Ore Geol Rev 39:101–115